IRAQI JOURNAL OF MATERIALS
Volume (3) Issue (3) July-September 2024, pp. 1-6

Effects of Annealing and Substrate Temperatures on Dielectric Properties of $CuInGaS_2$ Structures Prepared by Quenching-Assisted Vacuum Coating Technique

Ahmed M. Elgebali, Emad S. Sami, Basma A. Moharram

Department of Power and Energy Engineering, Faculty of Engineering, Minia University, Menia, EGYPT

Abstract
In this work, the effect of substrate temperature on some physical properties of CuInGaS2 thin films was studied. The frequency and temperature dependencies upon AC conductivity were studied in the range 100Hz-10MHz and temperature range of 30-180°C. The AC activation energy was found to increase with increasing substrate temperature from 20 to 150°C and to decrease with increasing frequency from 100 Hz to 100 MHz. A nonsystematic sequence was shown with the increment of substrate temperature. According to these results, there is a strong relation between the preparation or substrate temperature and heat treatment as they have sufficient effects on the physical properties of the quaternary compound thin films.

Keywords: $CuInGaS_2$ semiconductor; Thin films; Heterojunction; Activation energy
Received: 15 February 2024; **Revised:** 16 May 2024; **Accepted:** 23 May 2024; **Published:** 1 July 2024

1. Introduction
Recently, many quaternary materials have been extensively explored and invented for requiring a better performance of photonic and optoelectronic devices, such as $CuInGaS_2$, CuInGaSe, CuInSeTe, CuInSTe, ZnInSnO, InGaZnO, CuZnSnTe and CuZnSnSe [1-8]. Particularly, $CuInGaS_2$ possesses Cu_2S and InGa characteristics that can be applied in many fields of photonics and optoelectronics [9]. This study uses multi-compound $CuInGaS_2$ material and applies in channel layer of thin-film transistors (TFTs). Many different Cu_2S-based TFTs became emerging devices and strongly expected to replace conventional silicon TFTs because of their good device performance, and potential for transparent and flexible active circuits [10,11]. However, the composition of Cu_2S-based crystallization is not stable enough that can affect the performance of TFTs. The additional indium and tin doping promoted a more stable equilibrium the $CuInGaS_2$ matrix that can help the performance of the optoelectronics devices improvement [12].

Quaternary compounds are considered as absorbing materials for solar cell applications. There are few data available about their bulk material properties [13-15] as well as thin films [16-19]. The available data refer that there is a strong dependence between their structure and preparation conditions, which may be due to the amorphous nature as well as the dependencies of their properties on the ambient conditions. The electrical and optical properties of $CuInGaS_2$, CuInGaSe, CuInSeTe and CuInSeS thin films were determined and studied [20,21].

$CuInGaS_2$ adopts the chalcopyrite structure similar to high-efficiency $CuInGaSe_2$. Despite the high photoconversion efficiency of 23.35% achieved using $CuInGaS_2$, the certified record PCE of pure sulfide solar cells remained limited to 15.5% thus far. Hence, determining the losses and their underlying origin is of paramount importance to improve the understanding and, consequently, the performance of pure sulfide $CuInGaS_2$ chalcopyrite [22]. A good solar absorber material requires an efficient generation of photocarriers followed by a sustained build-up of charge-carrier density [23]. The latter is directly correlated to quasi-Fermi level splitting (QFLS) and charge-carrier lifetime, often used to analyze the

© All Rights Reserved

absorber quality [24,25]. Non-radiative recombination losses reduce the maximum achievable QFLS and lifetime, increasing photo-voltage deficit. The PCE for $CuInGaS_2$ has remained limited for a long time, mainly due to a large photo-voltage deficit. Moreover, rather low QFLS and short charge-carrier lifetimes (~hundreds of ps) are typically observed for $CuInGaS_2$. This implies significant non-radiative recombination in $CuInGaS_2$. The origin of non-radiative recombination lies in both bulk and interface (front and back-contact) defects [26-28].

This work presents the synthesis of quaternary alloy of $CuInGaS_2$ and then preparation of thin films at various substrate temperatures and point out the dependencies of dielectric and structural properties on deposition condition using relation between the preparation temperature and these properties.

2. Experimental Work

The alloys of $CuInGaS_2$ were prepared by quenching technique. The exact amount of high purity (99.99%) copper (Cu), indium (In), gallium (Ga) and sulfur (S) elements, in accordance with their percentages, are used. The mixed elements are sealed in evacuated (~10^{-3} Torr) quartz ampoule (25 cm in length and 8 mm internal diameter). Ampoules containing the elements were heated up to 1000 °C and frequently rocked at the highest temperature for 10 hours. The quenching was done in water immediately after taking out the ampoules from the furnace. Edward vacuum coating system was used to deposit $CuInGaS_2$ films at different substrate temperatures (30, 100 and 150 °C).

Aluminum electrodes with thickness of 200 nm were deposited on each adjacent surfaces of specimen by thermal evaporation technique under pressure of 10^{-5} Torr using an Edward E306A coating unit. The specimen was fixed in a holder and placed into a Heresies electronic temperature-controlled oven. High and low holder terminals are connected to a Hewlett-Packard HP4274A dielectric analyzer, the third holder terminal was connected to the earth. The dielectric parameters like total resistance (R_T), total capacitance (C_T) and dissipation factor (tanδ) were measured (in parallel mode) under certain frequency range 10^2-10^6 Hz. The AC conductivity (σ_{AC}) has been estimated from the obtained dielectric data using the following relation [29]:

$$\varepsilon_2 = \frac{\sigma_{AC}}{\varepsilon_0} \quad (1)$$

where the dielectric constants (ε_1 and ε_2) can be calculated using the following relation [29]:

$$\varepsilon_1 = \frac{C.t}{\varepsilon_0 A} \quad (2)$$

where C is the capacitance, ε_0 is the permittivity of free space, t is film thickness, is the angular frequency, A is the effective area for capacitance, and □AC is the AC conductivity given by [30]:

$$\sigma_{AC} = \omega\varepsilon_0\varepsilon_1 \tan\delta \quad (3)$$

where tanδ is the dielectric tangent loss

The conductivity measured with an AC technique is given by [30]:

$$\sigma(\omega,T) = \sigma_{dc}(T) + a(T)\omega^S \quad (4)$$

The first term $\sigma_{dc}(T)$ in Eq. (5) is the direct current or DC conductivity, ω=0, conductivity, while the second term a(T) is the temperature-dependence factor and "s" is an exponent in the range 0<s<1. This equation estimates that if the first term is less than the second term, then $\sigma(\omega,T)\propto\omega^s$, so that the plot diagram of σ versus log(ω) is a straight line with slope s. While if the first term is larger than the second term (with increasing temperature), then the plot of σ versus ω in log scale should give a horizontal straight-line.

3. Results and Discussion

Figure (1) shows the SEM images of the as-deposited $CuInGaS_2$ thin films deposited on substrates of different temperatures (20, 100 and 150°C). It is clear that the particle size on the surface is decreasing with increasing substrate temperature. This can be attributed to the effect of substrate temperature to diffuse the deposited particles into smaller ones before finally deposit over the substrate. This reduction in the particle size may have reasonable effect on the physical properties of these films, mainly conductivity and dielectric constant. However, increasing substrate temperature should be carefully chosen to produce $CuInGaS_2$ thin films with required properties and characteristics for certain uses and applications.

Figure (2) shows the dependency of angular frequency on total conductivity $\sigma_{tot}(\omega)$ for the $CuInGaS_2$ thin films deposited at different substrate temperatures (20, 100 and 150°C) in the heat treatment range 30-180 °C. It is clear that there is proceeding increase of $\sigma_{tot}(\omega)$ that increased within the whole frequency range, i.e., the alternative (AC) conductivity, and the dominated or, σ_{DC} conductivity is much lesser than the σ_{AC}, which indicates that the electronic polarization and the conductivity is purely AC. Some uses and applications of quaternary semiconducting thin films, especially power electronics and

© All Rights Reserved

high-temperature photonics, require to determine such behavior within as much as stable range of varying temperatures.

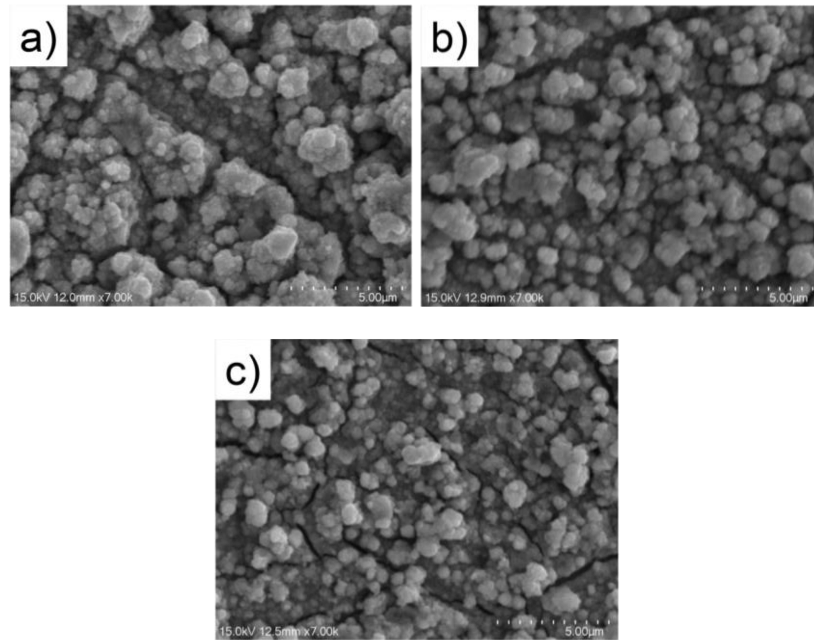

Fig. (1) SEM images of as-deposited $CuInGaS_2$ thin films deposited on substrates with temperature (a) 20°C, (b) 100°C, and (c) 150°C

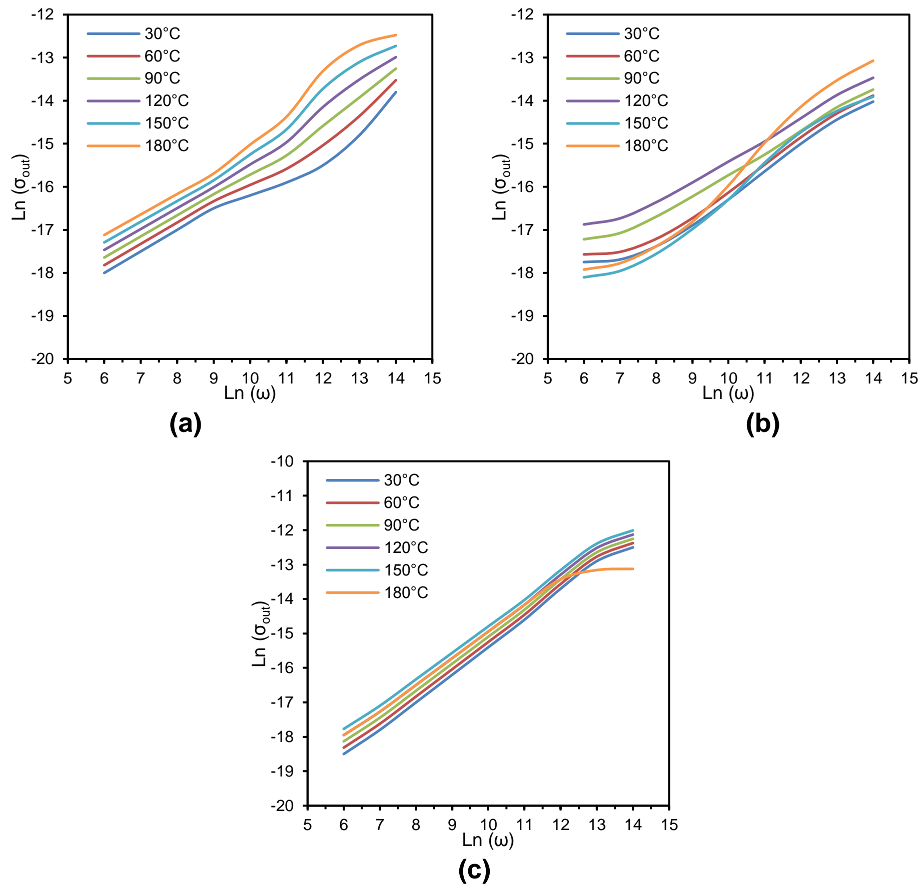

Fig. (2) Variation of $Ln(\sigma_{tot})$ with $Ln(\omega)$ for as-deposited $CuInGaS_2$ thin films and annealed at different temperatures for substrate temperature of (a) 20°C, (b) 100°C, and (c) 150°C

© All Rights Reserved

As shown in table (1), the exponent S, which is the slope of $dLn[\sigma_{tot}(\omega)]/d(\omega)$ decreases with increasing substrate temperature (T_S) in the low temperature range, while s increases at elevated temperatures, i.e., 150 °C, with increasing of T_S. The value of s increased with increasing heat treatment temperature of films deposited at T_S=100 °C. Also, s showed progress decreasing with oven temperature for samples deposited at 150 °C.

The AC activation energy, E_{AC}, for $CuInGaS_2$ films are estimated from the drawing of $Ln\sigma_{tot}(\omega)$ against the reciprocal absolute temperature, as indicated in Fig. (3).

Table (1) Values of s, τ and α for $CuInGaS_2$ thin films

T (°C)	As-deposited			T_S=373K			T_S=423K		
	S	τ x10^{-4} (s)	α	S	τ x10^{-4} (s)	α	S	τ x10^{-4} (s)	α
30	0.5853	-	0.1120	0.5348	-	0.3920 0.1792	0.9567	- 0.0398	0.2016 0.2800
60	0.6395	-	0.1456	0.5444	13.281	0.1904 0.1008	0.9291	- 0.0398	0.2240 0.2016
90	0.7131	-	0.1008	0.5089	13.281	0.1008 0.1680	0.9039	13.281 0.0398	0.1456 0.2800
120	0.7971	- 0.398	0.1232 0.0784	0.4638	-	0.2352	0.8634	- 0.0398	-
150	0.8341	- 0.159	0.0560 0.1120	0.6219	- 0.796	0.0672 0.0336	0.8451	- 0.0398	0.2240 0.1680
180	0.7911	-	0.1232 0.1120	0.7911	- 0.159	0.1680 0.1680	0.8152	- 0.0796	0.2240 0.2016

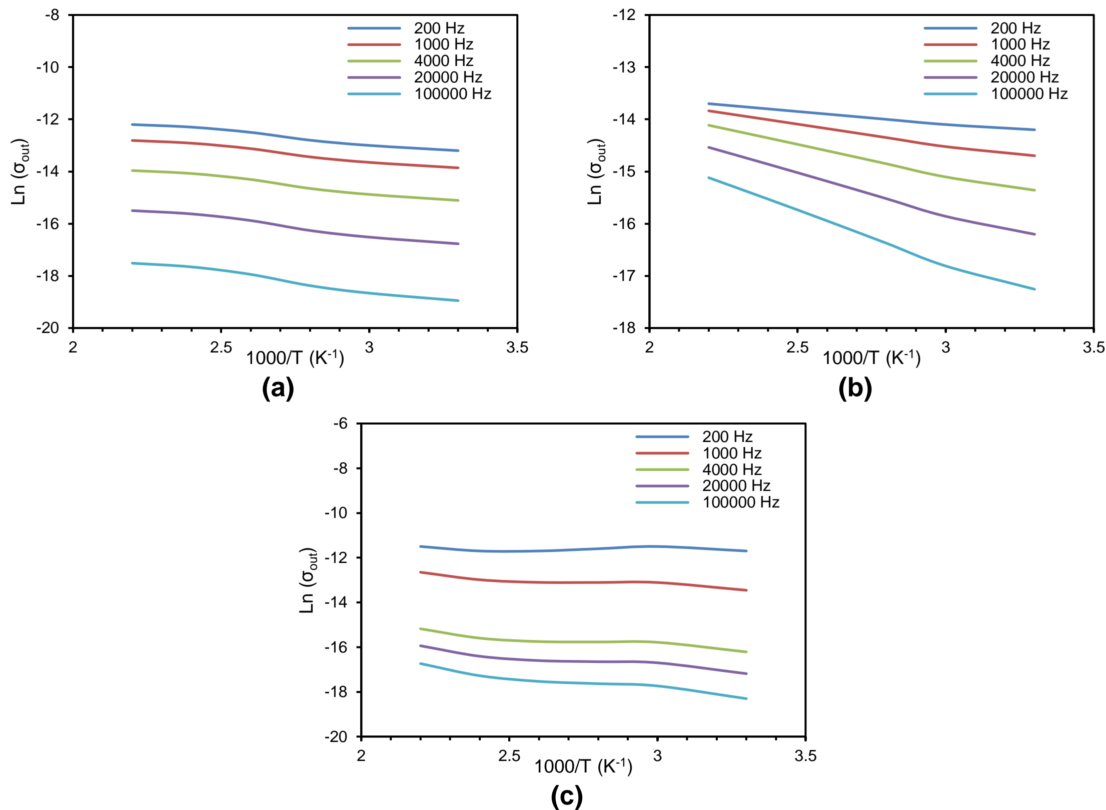

Fig. (3) Variation of $Ln(\sigma_{tot})$ with 1000/T for $CuInGaS_2$ thin films deposited at different substrate temperatures for substrate temperature of (a) 20°C, (b) 100°C, and (c) 150°C

Table (2) illustrates the E_{AC} values at selected frequencies (200 Hz, 1 kHz, 4 kHz, 10 kHz and 100 kHz). The results show that each sample declared one E_{AC}. On the other side, there is a direct relation between E_{AC} and frequency, while there is an inverse relation between E_{AC} and T_S. The E_{AC} decreases from 0.1132 to 0.0962 eV, while it increases from 0.1132 to 0.1258 eV with increasing frequency from 1 kHz to 100 kHz as well as increasing substrate temperature from 20 to 150 °C, respectively. The increase in frequency results in an increase of vibrating energy and hence the E_{AC} values will be decreased. This indicated that conductivity is purely AC, while the elimination of the localized states and

© All Rights Reserved

vacancies explained the increase of E_{AC} with increasing T_S. The presence of large amount of trapping states at the grain boundary was proposed that able to capture free charge carries [31]. These charged states at grain boundary create potential barriers, which oppose the passage of carriers from grain to neighboring ones, where their sites increase with increasing T_S, which resulted in decreasing conductivity or increasing E_{AC} values.

The real dielectric constant (ε_r) of $CuInGaS_2$ films prepared at different T_s, are measured within the employed frequency range (100Hz – 10MHz) as shown in Fig. (4). It is clearly from the ε_r pattern versus Log(ω), in Fig. (4) that the ε_r exhibits to increase with increasing heat treatment temperature, while it decreases with increasing frequency. This is ascribed to the fact that the electrode blocking layer is dominated, thus, the dielectric behavior is affected by the electrode polarization, while ε_r attained minimum values at high frequencies, which indicates that the dielectric signal is not affected by electrode polarization [8]. On the other hand, it is noticeable remarked that the values of ε_r, at frequency of 10^2 Hz, increase with increasing heat treatment and substrate temperatures. Indeed, the ε_r increases from 615 to 1064 and from 615 to 802 when heat treatment temperature increases from 30 to 180 °C and substrate temperature increases from 30 to 150 °C, respectively.

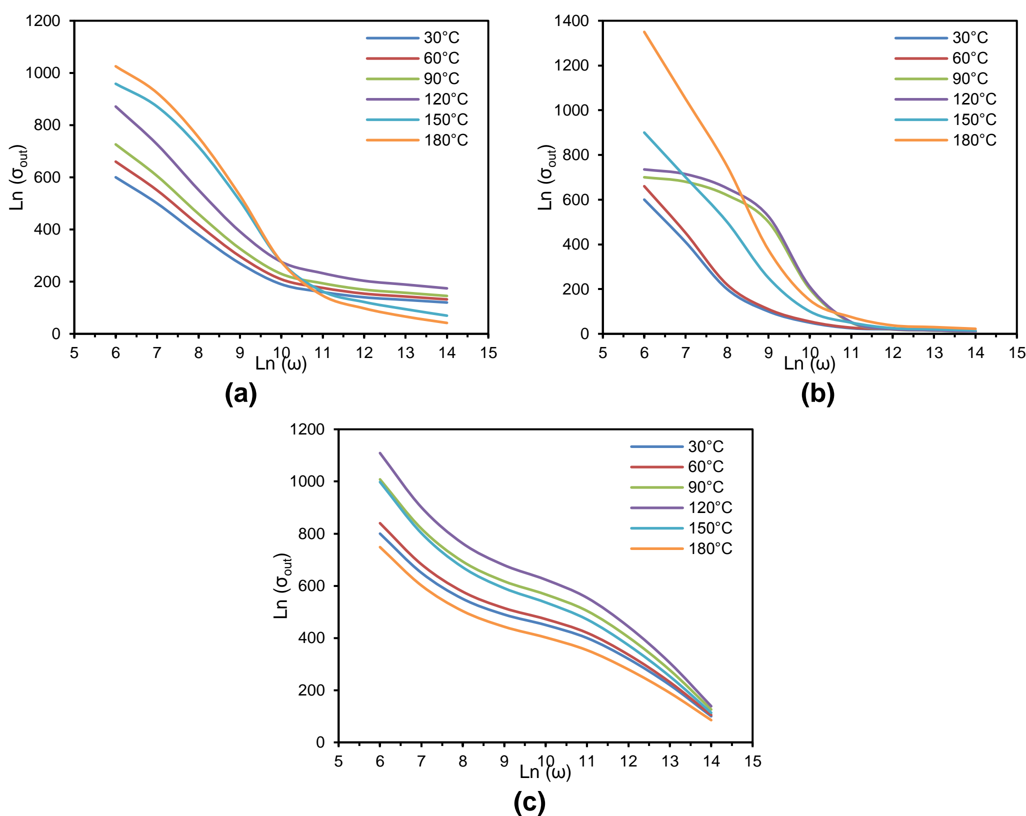

Fig. (3) Variation of ε_r with Lnω for as-deposited $CuInGaS_2$ thin films and annealed at different temperatures for substrate temperature of (a) 20°C, (b) 100°C, and (c) 150°C

Table (2) Values of E_{AC} for $CuInGaS_2$ thin films

Frequency (Hz)	E_{AC} (eV)		
	T_S (°C)		
	20	100	150
200	0.1132	0.1210	0.1258
1000	0.1115	0.1126	0.0517
4000	0.1022	0.1089	0.0336
10000	0.0973	0.0449	0.021
100000	0.0962	0.0103	0.0114

4. Conclusions

From the results obtained from this work, it can be concluded that the single phase with chalcopyrite structure of $CuInGaS_2$ becomes more pronounces at elevated temperatures. Also, similar variation

© All Rights Reserved

sequence declared by α and τ values with the increment of substrate and treatment temperatures. The increase of α and τ refer to reduction of intermolecular force, while reducing of α and τ refers to the rising of intermolecular force. It is evident from the polarizability values that $CuInGaS_2$ thin films can be used as resistor in electronic circuits.

References

[1] B.A. Hasan and D.A. Umran, "Dielectric permittivity and ac conductivity of CuInSeTe thin films", Semicond. Sci. Technol. 27 (2012) 125014.
[2] O.A. Hamadi, R.A. Markub and A.A.K. Hadi, "Heat-annealed enhanced-diffusion of silver in gallium arsenide", J Edu. Al-Mustansiriya Univ., 3 (2001) 35-44.
[3] B.A. Hasan, "AC Conductivity and dielectric analysis of CuInSSe Thin Films", Int. J. Thin Film Sci. Tech., 2(1) (2013) 29-36.
[4] O.A. Hamadi, K.Z. Yahiya and O.N.S. Jassim, "Properties of Silicon Carbide Thin Films Deposited by Vacuum Thermal Evaporation", J. of Semicond. Technol. Sci., 5(3) (2005) 182-186.
[5] R. Diaz, M. Leon and F. Reuda, "Characterization of Cu–In–Se–Te system in thin films grown by thermal evaporation," J. Vac. Sci. Technol. A, 10 (1992) 295-300.
[6] O.A. Hamadi and K.Z. Yahiya, "Optical and electrical properties of selenium-antimony heterojunction formed on silicon substrate", Sharjah Univ. J. Pure Appl. Sci., 4(2) (2007) 1-11.
[7] K. Inakoshi et al., "Preparation of $CuIn(S_xSe_{1-x})_2$ thin films by sulfurization and Selenization", Solar Energy Mater. Solar Cells, 50(1) (1998) 37-42.
[8] B.A.M. Badr, O.A. Hamadi and A.K. Yousif, "Measurement of thermooptic coefficient of semiconductors by single-beam scanning technique", Eng. Technol. J., 27(5) (2007).
[9] K. Subbaramiah and V. Sundara Raja, "Structural and optical properties of spray-deposited $CuIn(S_{1-x}Se_x)_2$ thin films", Thin Solid Films, 208 (1992) 247-251.
[10] O.A. Hamadi, "Characteristics of CdO-Si Heterostructure Produced by Plasma-Induced Bonding Technique", Proc. IMechE, Part L, J. Mater.: Design & Appl., 222 (2008) 65-71.
[11] T. Ohashi et al., "$CuIn(S_xSe_{1-x})_2$ Thin Films by Sulfurization", Jap. J. Appl. Phys., 34 (1995) 4159-4166.
[12] O.A. Hamadi, "Effect of Annealing on the Electrical Characteristics of CdO-Si Heterostructure Produced by Plasma-Induced Bonding Technique", Iraqi J. Appl. Phys., 4(3) (2008) 34-37.
[13] S. Kuranouchi and T. Nakazawa, "Study of one-step electrodeposition condition for preparation of $CuIn(Se,S)_2$ thin films", Solar Energy Mater. Solar Cells, 50 (1998) 31-36.
[14] A.A.K. Hadi and O.A. Hamadi, "Optoelectronic Characteristics of As-doped Si Photodetectors Produced by LID Technique", Iraqi J. Appl. Phys. Lett., 1(2) (2008) 23-26.
[15] L.I. Soliman and T.A. Hendia, "Influence of γ-irradiation on the optical and electrical properties of $ZnIn_2Se_4$ films", Rad. Phys. Chem., 50(2), 1997, 175-177.
[16] O.A. Hamadi, N.J. Shakir and F.H. Hussain, "Magnetic Field and Temperature Dependent Measurements of Hall Coefficient in Thermal Evaporated Tin-Doped Cadmium Oxide Thin Films", Bulg. J. Phys., 37(4) (2010) 223-231.
[17] L. Soliman, T. Hendlia and H. Zayed, "Effect of annealing on the switching properties of CuInSeTe thin films", Fizika A (Zagreb), 16(1) (2007) 39-46.
[18] O.A. Hamadi, "Profiling of Antimony Diffusivity in Silicon Substrates using Laser-Induced Diffusion Technique", Iraqi J. Appl. Phys. Lett., 3(1) (2010) 23-26.
[19] C. Landry, J. Lockwood and R. Barron, "Synthesis of Chalcopyrite Semiconductors and Their Solid Solutions by Microwave Irradiation", Chem. Mater. 7(4) (1995) 699-706.
[20] O.A. Hammadi and M.S. Edan, "Temperature Dependencies of Refractive Index and Optical Elasticity Coefficient on Lens Induced in Nd:YAG Crystal", Iraqi J. Appl. Phys., 8(1) (2012) 35-41.
[21] J.Y.W. Seto, "Deposition of Polycrystalline Silicon by Pyrolysis of Silane in Argon", J. Electrochem. Soc., 122(5) (1975) 701-706.
[22] O.A. Hammadi, "Photovoltaic Properties of Thermally-Grown Selenium-Doped Silicon Photodiodes for Infrared Detection Applications", Phot. Sen., 5(2) (2015) 152-158.
[23] S. Kumar et al., "Growth and Characterization of Copper, Indium and Copper- Indium Alloy Films non-aqueous Method of Electro Deposition", Indian J. Pure Appl. Phys., 46 (2008) 198-203.
[24] O.A. Hammadi and N.E. Naji, "Electrical and spectral characterization of CdS/Si heterojunction prepared by plasma-induced bonding", Opt. Quantum Electron., 48(8) (2016) 375-381.
[25] A.K. Jonscher, "Review Article: Dielectric relaxation in solids", J. Phys. D: Appl. Phys., 32(14) (1999) R57-R70.
[26] O.A. Hammadi, "Characteristics of Heat-Annealed Silicon Homojunction Infrared Photodetector Fabricated by Plasma-Assisted Technique", Phot. Sen., 6(4) (2016) 345-350.
[27] Z. Ahmad, **"Polymeric Dielectric Materials"**, Ch. 1 (2014) p. 4, doi: 10.5772/50638.
[28] O.A. Hamadi, "Characterization of SiC/Si Heterojunction Fabricated by Plasma-Induced Growth of Nanostructured Silicon Carbide Layer on Silicon Surface", Iraqi J. Appl. Phys., 12(2) (2016) 9-13.
[29] R. Bari and L. Patil, "Chemically Deposited n-$CuInSe_2$/Polyiodide Based PEC Solar Cells", Sensors and Transducers, 125 (2011) 213-219.
[30] O.A. Hammadi, "Synthesis and Characterization of Polycrystalline Carbon Nitride Nanoparticles by Fast Glow Discharge-Induced Reaction of Methane and Ammonia", Adv. Sci. Eng. Med., 11(5) (2019) 346-350.
[31] S. Sze and K. Kwok, **"Physics of Semiconductor Devices"**, 3rd ed., John Wiley & Sons, Inc. (NJ, 2007).

© All Rights Reserved